

The Neutron Electric Dipole Moment and CP-violating Couplings
in the Supersymmetric Standard Model without R -parity

Darwin Chang^a, We-Fu Chang^a, Mariana Frank^b, and Wai-Yee Keung^c

^a*NCTS and Physics Department, National Tsing-Hua University,*

Hsinchu 30043, Taiwan, R.O.C.

^b*Concordia University, Montreal, Quebec, Canada, H3G 1M8*

^c*Physics Department, University of Illinois at Chicago, IL 60607-7059, USA*

Abstract

We analyze the neutron electric dipole moment (EDM) in the Minimal Supersymmetric Model with explicit R -parity violating terms. The leading contribution to the EDM occurs at the 2-loop level and is dominated by the chromoelectric dipole moments of quarks, assuming there is no tree-level mixings between sleptons and Higgs bosons or between leptons and gauginos. Based on the experimental constraint on the neutron EDM, we set limits on the imaginary parts of complex couplings λ'_{ijk} and λ_{ijk} due to the virtual b -loop or τ -loop.

The minimal supersymmetric standard model (MSSM) [1] has been widely considered as a leading candidate for new physics beyond Standard Model. However, unlike the standard model, supersymmetry allows renormalizable interactions which break R -parity defined as $(-1)^{3B+L+F}$ and violate the lepton and/or the baryon numbers. It is in fact one of the main theoretical weaknesses of these models because R -parity conservation is an ad hoc imposition which may or may not have a fundamental theoretical basis. Therefore, instead of neglecting them completely, it is interesting to ask how small these R -parity breaking (\mathcal{R}) couplings could be by investigating directly phenomenological constraints[2].

The most general renormalizable R -violating superpotential using only the MSSM superfields is

$$W_{\mathcal{R}} = \lambda_{ijk} L_i L_j E_k^C + \lambda'_{ijk} L_i Q_j D_k^c + \lambda''_{ijk} U_i^c D_j^c D_k^c + \mu_j L_j H_2 . \quad (1)$$

Here, i, j, k are generation indices. The couplings λ_{ij}^k and $\lambda_{ij}^{k''}$ must be antisymmetric in flavor, $\lambda_{ijk} = -\lambda_{jik}$ and $\lambda'_{ijk} = -\lambda'_{ikj}$. There are 36 lepton number non-conserving couplings (9 of the λ type and 27 of the λ' type) and 9 baryon number non-conserving couplings (all of the λ'' type) in Eq.(1). To avoid rapid proton decay, it is usually assumed in the literature that λ , λ' type couplings do not coexist with λ'' type couplings. This can be achieved easily by imposing baryon number symmetry. The bilinear terms $\mu_j L_j H_2$ contribute to lepton flavor and number violation and could be responsible for neutrino masses. Phenomenologically, many of these couplings have been severely constrained using low-energy processes or using high energy data at the colliders [3]–[10]. In this paper, we shall not consider λ''_{ijk} and μ_j couplings.

However, most of the bounds in the literature constrain the real part of the trilinear couplings, or the product of trilinear couplings. The exception is the bound coming from the ϵ_K which constrains $\text{Im}(\lambda'_{i12} \lambda'^*_{i21}) < 8 \times 10^{-12}$ [11]. We propose to study the neutron electric dipole moment, which is tightly bound by experiment, and thus obtain limits on the imaginary parts of different products of trilinear couplings from the ones imposed by ϵ_K .

The electric dipole moment of an elementary fermion is defined through its electromagnetic form factor $F_3(q^2)$ in the (current) matrix element:

$$\langle f(p') | J_\mu(0) | f(p) \rangle = \bar{u}(p') \Gamma_\mu(q) u(p), \quad (2)$$

where $q = p' - p$ and

$$\Gamma_\mu(q) = F_1(q^2)\gamma_\mu + \frac{F_2(q^2)}{2m}i\sigma_{\mu\nu}q^\nu + F_A(q^2)(\gamma_\mu\gamma_5q^2 - 2m\gamma_5q_\mu) + \frac{F_3(q^2)}{2m}\sigma_{\mu\nu}\gamma_5q^\nu, \quad (3)$$

with m the mass of the fermion and $F_1(0) = e_f$. The electric dipole moment (EDM) of the fermion field f is then given by

$$d_f = \frac{eF_3(0)}{2m}, \quad (4)$$

corresponding to the effective dipole interaction

$$\mathcal{L}_{\text{EDM}} = -\frac{i}{2}d_f\bar{f}\sigma_{\mu\nu}\gamma_5fF^{\mu\nu}. \quad (5)$$

In the static limit this corresponds to an effective Lagrangian $\mathcal{L}_{\text{EDM}} \rightarrow d_f\Psi_A^\dagger\vec{\sigma}\cdot\vec{E}\Psi_A$, where Ψ_A is the large component of the Dirac field. Similarly the quark chromoelectric dipole moment (CEDM) is the coefficient d_q^g in the effective operator:

$$\mathcal{L}_{\text{CEDM}} = -\frac{i}{2}d_q^g\bar{q}\sigma_{\mu\nu}\gamma_5\frac{\lambda^a}{2}qG^{a\mu\nu}. \quad (6)$$

The relevant Lagrangian for generating an EDM is:

$$\mathcal{L} = -\left(\frac{1}{2}\sum_{ij}\Psi_i\frac{\partial^2 W}{\partial\phi_i\partial\phi_j}\Psi_j + \text{H.c.}\right) + \dots = [\lambda'_{ijk}(-\tilde{\ell}_i u_j d_k^c + \tilde{\nu}_i d_j d_k^c) + \text{H.c.}] + \dots \quad (7)$$

It has been shown [4] that there is no one-loop contributions to EDMs based on λ , λ' or λ'' couplings based on helicity properties and symmetry. Here we briefly review its origin. It is easy to show that one cannot induce EDMs from the diagram that requires the external mass insertion due to the equation of motion. As a result of this lemma, proper helicities for external fermion lines have to come directly from vertices. Let us look at the electron EDM, which needs external L and E^c . For the correct quantum number, possible one loop contributions have to be proportional to either (1) $\lambda\lambda^*$ or (2) $\lambda'\lambda'^*$. Based on the above lemma, the external L and E^c are required to come directly from vertices. Case (1) cannot produce the helicity flip. Case (2) is even worse, there is no vertex to give E^c . So the one-loop electron EDM is absent. For the d quark EDM, possibilities are either (1) $\lambda'\lambda'^*$ or (2) $\lambda''\lambda''^*$. Case (1) does not work because both d_L and d^c have to come from a CP -even product of a complex conjugated pair of vertices, and case (2) fails badly because there is no vertex to give an external d_L . Similar reason follows for

the u quark EDM. As a reminder, there are one-loop EDM amplitudes [12] related to the bilinear term $\mu_j L_j H_2$, which mixes sleptons and Higgs bosons etc. We do not consider these couplings μ_i in this work.

At the two-loop level, a number of different types of configurations contribute, which we classify as rainbow-like (I), overlapping (II), tent-like (III) and Barr-Zee (IV)[13] types. The rainbow-like graphs (I) are those with two concentric boson loops, the outer of which must be a charged Higgs loop (for the same reason that 1-loop graphs do not exist). The inner loop may be a left or right sfermion. The complete set of this type of graphs is given in Fig. 1a. The complete set of overlapping type of graphs is given in Fig. 1b. In this case, one of them must be a charged Higgs, the other a left or right sfermion.

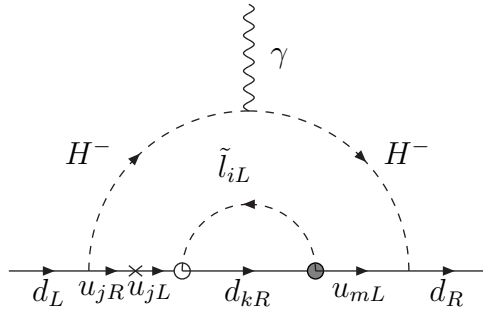


Fig. 1a (i) Rainbow-like diagram for the d quark. The generic $/R$ vertex is marked by \circ and its complex conjugate by \bullet .

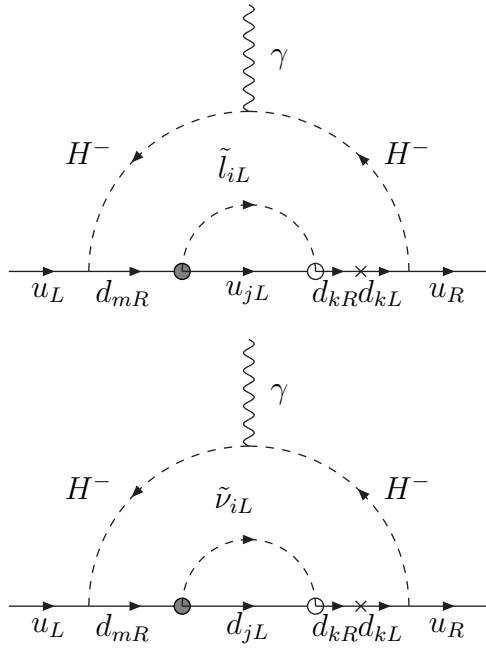


Fig. 1a (ii) Rainbow-like diagram for the u quark.

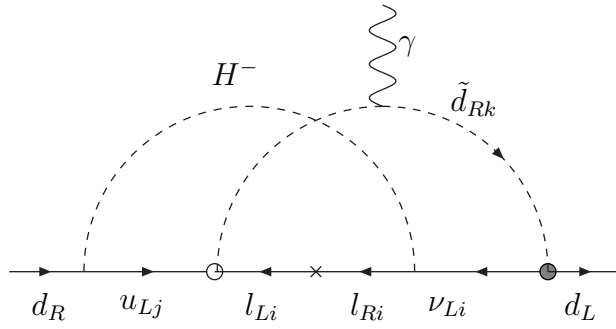


Fig. 1b (i) Overlapping diagram for the d quark using λ' .

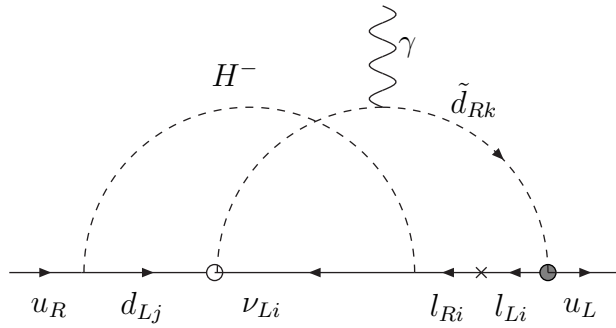


Fig. 1b (ii) Overlapping diagram for the u quark using λ' .

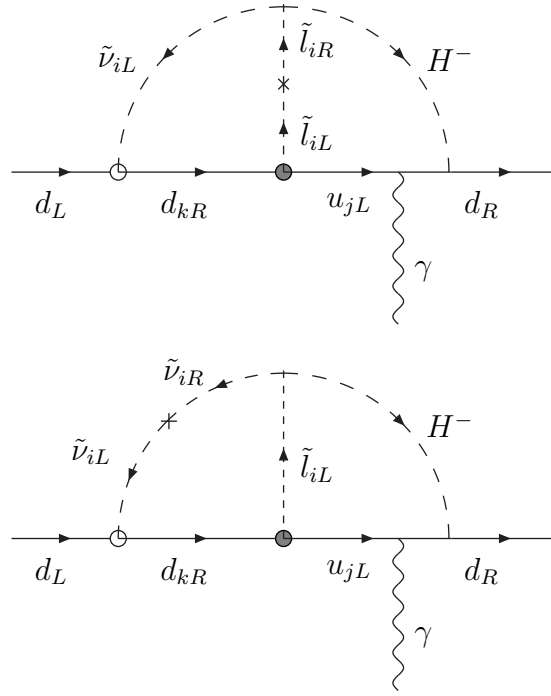


Fig. 1c (i) Tent-like diagram for the d quark using λ' .

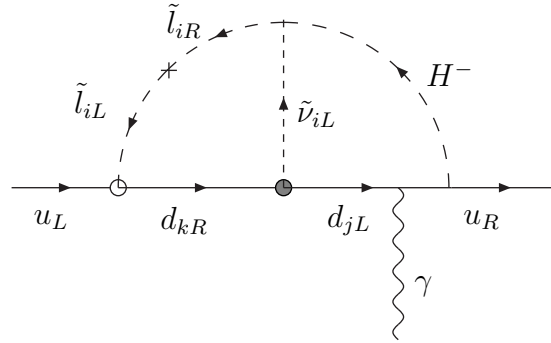


Fig. 1c (ii) Tent-like diagram for the u quark using λ' .

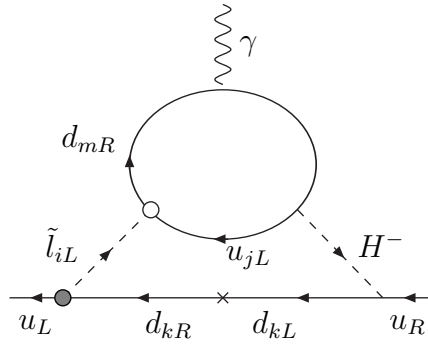


Fig. 1d Barr-Zee type graph for u quark EDM

The tent-like graphs (III) have a trilinear bosonic vertex. Again, the 3 different boson legs can be two sfermions and one charged Higgs (in all possible configurations). The complete set of this type of graphs is given in Fig. 1c. Careful consideration of all the type I–III graphs shows that their contributions are suppressed by both one power of light quark mass plus some CKM mixing angles factor compared to those of type IV (Fig. 2). Therefore, one expects the Barr-Zee type of contributions dominate and we shall study them in detail next.

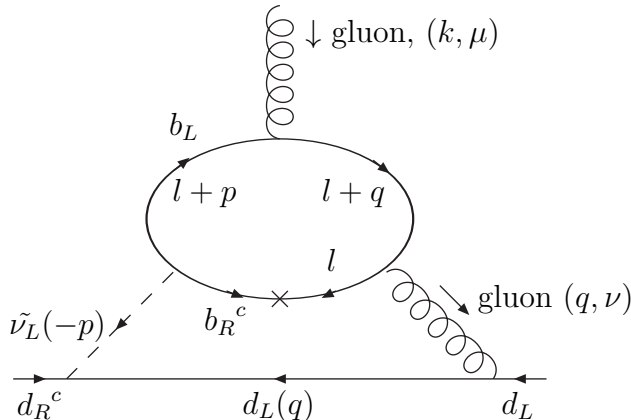


Fig. 2 A typical two-loop diagram of the Barr-Zee type. Note that there are 3 ways to insert mass.

In Ref. [4], only a rough estimate of the two-loop contributions to EDMs is provided. We shall present here a complete calculation of the quark (or electron) EDM and the quark CEDM at the two-loop level due to the Barr-Zee type mechanism and show that the neutron EDM is dominated by the CEDM of the d quark. This calculation leads to more stringent bounds than previously obtained.

There is another class of Barr-Zee graphs with sneutrino line replaced by the charged slepton line and corresponding modifications of the fermions charges in the loop. The calculations of these type of graphs are very similar to the one in the charged Higgs models of CP violation as in Ref.[14, 15]. Comparing the charged Higgs contributions to the EDM in Ref.[14, 15] with the neutral Higgs contributions given in Ref.[13], one can observe that the neutral Higgs contributions generally dominates given comparable coupling constants and boson masses. Therefore, we shall only give details of sneutrino contributions here.

$\tilde{\nu}gg$ vertex of the inner loop

The two-loop diagram to the CEDM of the d -type quark can appear with the coupling λ'_{ijk} through the virtual vertex $\tilde{\nu}gg$. The amplitude of the inner loop in terms of the leading gauge invariant terms is:

$$\Gamma^{\mu\nu} = S(q^2)[k^\nu q^\mu - k \cdot q g^{\mu\nu}] + P(q^2)[i\epsilon^{\mu\nu\alpha\beta} p_\alpha q_\beta], \quad (8)$$

where S and P correspond to scalar and pseudoscalar form factors respectively:

$$\begin{aligned} S(q^2) &= \frac{m_b g_s^2 \lambda'_{i33}}{16\pi^2} \int_0^1 dy \frac{1 - 2y(1-y)}{m_b^2 - y(1-y)q^2}, \\ P(q^2) &= \frac{m_b g_s^2 \lambda'_{i33}}{16\pi^2} \int_0^1 dy \frac{1}{m_b^2 - y(1-y)q^2}. \end{aligned}$$

Second loop

Combining the two twisted diagrams and the two choices of sneutrino flow directions, we have a combinatoric factor of 4 in the the two loop CEDM amplitude. In the convention of Eqs.(2–6), we obtain the CEDM of the d quark at the scale of m_b ,

$$\begin{aligned} \left(\frac{d_d^g}{g_s}\right)_{m_b} &= \frac{m_b g_s^2 |_{m_b}}{128\pi^4} \text{Im}(\lambda'_{i33} \lambda'_{i11}) \int_0^1 dy \int_0^\infty \frac{Q^2 d(Q^2)(1-y(1-y))}{(m_b^2 + y(1-y)Q^2)(Q^2 + M_{\tilde{\nu}_i}^2)Q^2} \\ &= \frac{\alpha_s \text{Im}(\lambda'_{i33} \lambda'_{i11})}{32\pi^3} \frac{m_b}{M_{\tilde{\nu}_i}^2} \cdot F\left(\frac{m_b^2}{M_{\tilde{\nu}_i}^2}\right), \end{aligned} \quad (9)$$

with the loop function

$$F(\tau) = \int_0^1 dy \frac{(y^2 - y + 1)}{y(1-y) - \tau} \ln\left(\frac{y(1-y)}{\tau}\right) \quad (10)$$

$$\rightarrow \frac{\pi^2}{3} + 2 + \ln \tau + (\ln \tau)^2 \quad \text{for } \tau \rightarrow 0. \quad (11)$$

Implicit sum over sneutrino flavors i is assumed in the above. The last asymptotic form is useful because the ratio $\tau = m_b^2/M_{\tilde{\nu}_i}^2$ is small. The large logarithmic factor helps place a strong constraint on λ' couplings. Note that sneutrino is the heaviest particle in the loop. At m_b scale, the sneutrino induces a four fermion interaction of b and d quarks. As a result, by simple power counting, the gluonic loop is logarithmically divergent which explains the large logarithmic enhancement factor.

Replacing the gluon line by the photon line, we obtain the EDM of the quark simply by substituting the color factor and the charge factor.

$$\left(\frac{d_d^\gamma}{e}\right)_{m_b} = 6e_d e_b^2 \left(\frac{\alpha_{\text{em}}}{\alpha_s}\right)_{m_b} \left(\frac{d_d^g}{g_s}\right)_{m_b}. \quad (12)$$

Now we address the QCD evolution of these Wilson's coefficients. As an effective theory, the 4-fermion vertices of the form $(\bar{b}b)(\bar{d}d)$ arise first in the energy scale below $M_{\tilde{\nu}_i}$ when $\tilde{\nu}$ are integrated out of the theory. Then the EDM and the CEDM of the d quark arise below m_b scale. Therefore, the λ' couplings in the above equations are evaluated at the m_b scale. We ignore the dressing of these 4-fermion vertices because of the small value of their couplings and the slow running of α_s at such high energy scale. In this perspective, the λ' factors in Eq. (9) are defined at the short distance scale near $M_{\tilde{\nu}}$. Below m_b , the CEDM and the EDM of light quarks appear and they evolve down to the hadronic scale Λ_H by

$$\left(\frac{d_d^g}{g_s}\right)_{\Lambda_H} / \left(\frac{d_d^g}{g_s}\right)_{m_b} = \left(\frac{g_s(m_b)}{g_s(m_c)}\right)^{\frac{4}{25}} \left(\frac{g_s(m_c)}{g_s(\Lambda_H)}\right)^{\frac{4}{27}} = Z^g, \quad (13)$$

$$\left(\frac{d_d^\gamma}{e}\right)_{\Lambda_H} / \left(\frac{d_d^\gamma}{e}\right)_{m_b} = \left(\frac{g_s(m_b)}{g_s(m_c)}\right)^{\frac{8}{25}} \left(\frac{g_s(m_c)}{g_s(\Lambda_H)}\right)^{\frac{8}{27}} = Z^\gamma. \quad (14)$$

Note that in some references [17], a light quark mass coefficient has been factored out so that the form of evolution equation looks different from above. We denote by D_n^g (D_n^γ) the neutron EDM due to the CEDM (EDM) of light quarks. The $SU(6)$ relation gives:

$$\frac{D_n^g}{e} = \left[\frac{4}{9} \left(\frac{d_d^g}{g_s}\right)_{\Lambda_H} + \frac{2}{9} \left(\frac{d_u^g}{g_s}\right)_{\Lambda_H} \right]. \quad \frac{D_n^\gamma}{e} = \left[\frac{4}{3} \left(\frac{d_d^\gamma}{e}\right)_{\Lambda_H} - \frac{1}{3} \left(\frac{d_u^\gamma}{e}\right)_{\Lambda_H} \right]. \quad (15)$$

For $\alpha_s(M_Z) = 0.12$ and $g_s(\Lambda_H)/(4\pi) = 1/\sqrt{6}$, the QCD evolution factors Z^γ and Z^g are about 0.71 and 0.84 respectively. Our formulas and numerical values are consistent with those in Ref. [17] but differ from those in Ref. [18].

For completeness, we add another large contribution to the d quark EDM due to the τ -lepton replacing the b quark inside the first loop. We obtain two independent contributions as:

$$\left(\frac{d_d^\gamma}{e}\right)_{m_b} (b\text{-loop}) = -\frac{\alpha_{\text{em}}}{16\pi^3} \sum_{i=1,2,3} \frac{3e_d e_b^2 m_b}{M_{\tilde{\nu}_i}^2} \text{Im}(\lambda_{i33}^* \lambda'_{i11}) \cdot F\left(\frac{m_b^2}{M_{\tilde{\nu}_i}^2}\right), \quad (16)$$

$$\left(\frac{d_d^\gamma}{e}\right)_{m_\tau}(\tau\text{-loop}) = -\frac{\alpha_{\text{em}}}{16\pi^3} \sum_{i \neq 3} \frac{e_d m_\tau}{M_{\tilde{\nu}_i}^2} \text{Im}(\lambda_{i33}^* \lambda'_{i11}) \cdot F\left(\frac{m_\tau^2}{M_{\tilde{\nu}_i}^2}\right) . \quad (17)$$

The latter contribution from the τ -loop is induced at the m_τ scale and we need to adjust the minor change in the QCD evolution. There are also other Barr-Zee type diagrams from the exchange of W^\pm or Z gauge bosons. However, they are known to be giving smaller contributions and thus we ignore them in our numerical study [14, 15, 16].

As u_R is not directly involved in the \mathcal{R} interaction, the u quark CEDM do not appear through λ' in the form of Fig. 2. Nonetheless, there are two-loop diagrams Fig. 1a (ii), 1b(ii), 1c(ii) and 1d which are suppressed by the light quark mass and mixing angles. Therefore, the \mathcal{R} contribution to the neutron EDM is dominated by the d quark CEDM and EDM. Assuming all $M_{\tilde{\nu}_i}$ are equal and taking typical values, $M_{\tilde{\nu}_i} \approx 300$ GeV and $m_b \approx 4.5$ GeV, we have

$$D_n^g \simeq 5.46 \times 10^{-21} \text{ (e-cm)} \times \sum_i \text{Im}(\lambda_{i33}^* \lambda'_{i11}) , \quad (18)$$

$$\begin{aligned} D_n^\gamma \simeq & -1.03 \times 10^{-22} \text{ (e-cm)} \times \sum_i \text{Im}(\lambda_{i33}^* \lambda'_{i11}) \\ & -1.92 \times 10^{-22} \text{ (e-cm)} \times \sum_{i \neq 3} \text{Im}(\lambda_{i33}^* \lambda'_{i11}) . \end{aligned} \quad (19)$$

Our numerical result shows that the strongest constraint comes from the CEDM of the d quark. Using the up-to-dated experimental [19] bound $|D_n| < 6.3 \times 10^{-26}$ e-cm and barring accidental cancellation among contributions, we derive the constraints:

$$\sum_i \text{Im}(\lambda_{i33}^* \lambda'_{i11}) < 1.2 \times 10^{-5} , \quad (20)$$

$$\sum_{i \neq 3} \text{Im}(\lambda_{i33}^* \lambda'_{i11}) < 33 \times 10^{-5} , \quad (21)$$

for $M_{\tilde{\nu}} = 300$ GeV.

In Fig. 3 we plot both the photon and gluon contributions to the neutron EDM versus the sneutrino mass $M_{\tilde{\nu}}$ in the region of interest (100 to 600 GeV) with $\sum_i \text{Im}(\lambda_{i33}^* \lambda'_{i11})$ or $\sum_{i \neq 3} \text{Im}(\lambda_{i33}^* \lambda'_{i11})$ scaled to 10^{-5} . One could see that the gluon contribution consistently dominates the corresponding photon one by at least an order of magnitude over the whole parameter space explored.

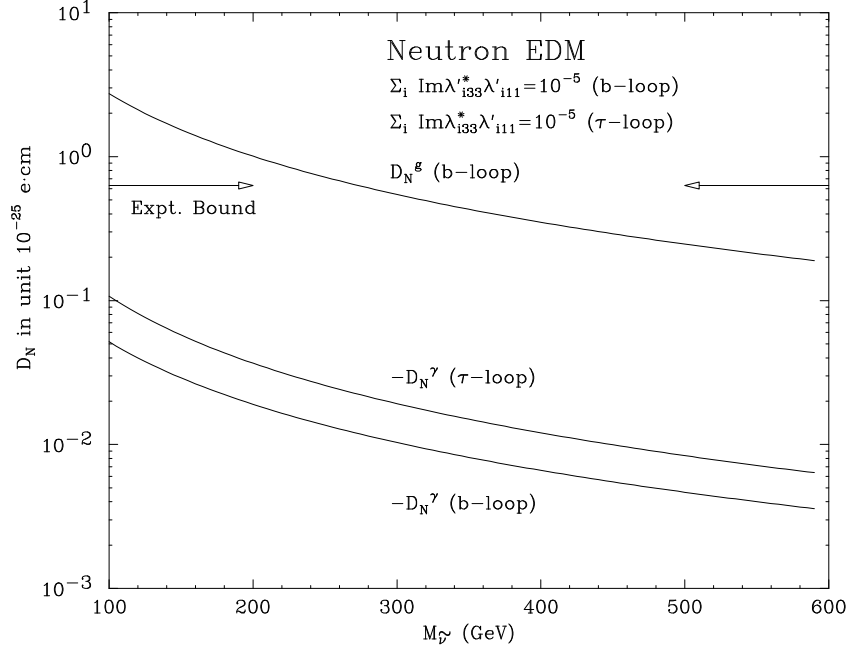


Fig. 3 The neutron EDM D_n versus $M_{\tilde{\nu}}$ with $\sum_i \text{Im}(\lambda'_{i33} \lambda'_{i11})$ or $\sum_i \text{Im}(\lambda_{i33} \lambda'_{i11})$ scaled to 10^{-5} .

The electron EDM can arise via both λ' or λ -type R -parity violating coupling Ref.[4]. Based on above study, the analytical formula for the electron EDM at the two-loop level is:

$$\left(\frac{d_e^\gamma}{e}\right) = -\frac{\alpha_{em}}{16\pi^3} \left[\sum_{i \neq 1} \frac{3e_b^2 m_b}{M_{\tilde{\nu}_i}^2} \text{Im}(\lambda'_{i33} \lambda_{i11}) \cdot F\left(\frac{m_b^2}{M_{\tilde{\nu}_i}^2}\right) + \frac{m_\tau}{M_{\tilde{\nu}_2}^2} \text{Im}(\lambda_{233} \lambda_{211}) \cdot F\left(\frac{m_\tau^2}{M_{\tilde{\nu}_2}^2}\right) \right]. \quad (22)$$

In Fig. 4 we assume all $M_{\tilde{\nu}_i}$ to be equal and plot contributions to the electron EDM versus the sneutrino mass $M_{\tilde{\nu}}$ in the region of interest (100 to 600 GeV). Using the up-to-dated experimental [20] bound $|d_e| < 0.43 \times 10^{-26}$ e-cm and barring from accidental cancellation among contributions, we derive constraints:

$$\text{Im}(\lambda_{233} \lambda_{211}) < 0.74 \times 10^{-5}, \quad (23)$$

$$\sum_{i \neq 1} \text{Im}(\lambda'_{i33} \lambda_{i11}) < 1.3 \times 10^{-5}, \quad (24)$$

for $M_{\tilde{\nu}} = 300$ GeV.

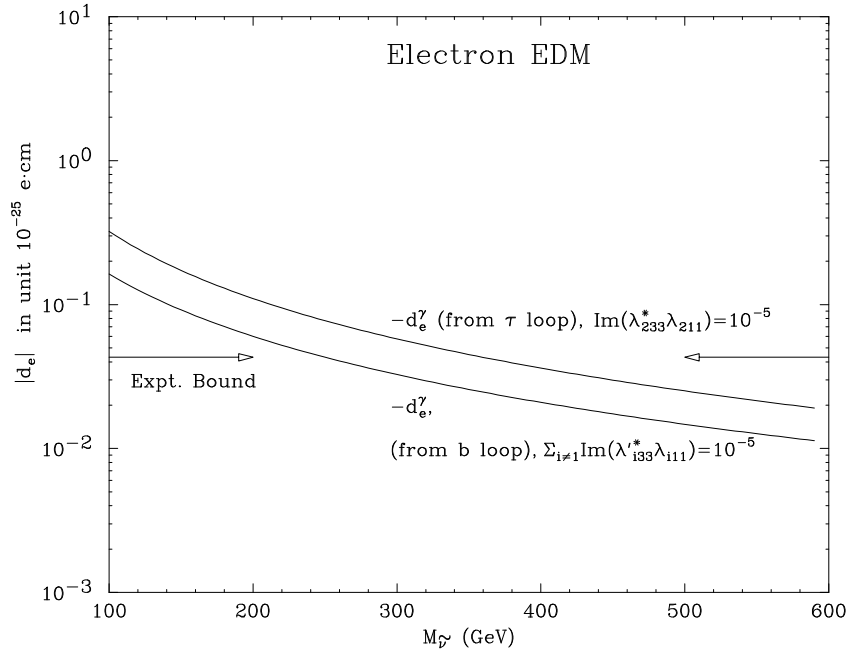


Fig. 4 The electron EDM d_e versus $M_{\tilde{\nu}}$.

Conclusion

We have presented an exact and complete calculation of the dominant contribution to the neutron EDM in a minimal supersymmetric model without R parity due to the couplings λ and λ' . The CP violation does not depend on the complex phases ϕ_μ and ϕ_{A_0} (the phases of the Higgsino mass parameter and the trilinear scalar coupling A_0) in Minimal Supergravity models, therefore unrelated to the restrictive bounds or complicated cancellations necessary in MSSM. The leading R contribution to the neutron EDM occurs at two-loop level through the Barr-Zee mechanism. We obtain stringent bounds on the product $\text{Im}\lambda_{i33}^* \lambda'_{i11} < \mathcal{O}(10^{-5})$.

Acknowledgments This work was supported in parts by National Science Council of R.O.C., by U.S. Department of Energy (Grant No. DE-FG02-84ER40173) and by NSERC of Canada (Grant No. SAP0105354). MF and WFC would like to thank the High Energy Physics Group at the University of Illinois at Chicago for their hospitality while this work was initiated.

References

- [1] H. P. Nilles, Phys. Rep. **110**, 1 (1984);
H.E. Haber and G.L. Kane, Phys. Rep. **117**, 75 (1985);
R. N. Mohapatra, Unification and Supersymmetry Springer Verlag (1991);
S. Dawson, hep-ph/9612229;
M. Drees, hep-ph/9611409;
M. Peskin, hep-ph/9705479; etc.
- [2] J. Ellis, et al., Phys. Lett. **B150**, 142 (1985);
G.G. Ross and J.W.F. Valle, Phys. Lett. **B151**, 375 (1985);
S. Dawson, Nucl. Phys. **B261**, 297 (1985);
S. Dimopoulos and L. Hall, Phys. Lett. **B207**, 210 (1987).
- [3] H. Dreiner, hep-ph/9707435 (1997);
G. Bhattacharyya, hep-ph/9709395 (1997);
B. Allanach *et al*, hep-ph/9906224 (1999).
- [4] R.M. Godbole, S. Pakvasa, S.D. Rindani and X.Tata, hep-ph/9912315 (1999);
S.A. Abel, A. Dedes and H.K. Dreiner, hep-ph/9912429 (1999).
- [5] L. Hall and M. Suzuki, Nucl. Phys. **B231**, 419 (1984);
R.N. Mohapatra, Phys. Rev. **D 34**, 909 (1986);
V. Barger, G.F. Giudice and T. Han, Phys. Rev. **D40**, 2987 (1989);
R. Godbole, P. Roy and X. Tata, Nucl. Phys. **B401**, 67 (1993);
M. Hirsch, H.V. Klapdor-Kleingrothaus and S.G. Kovalenko, Phys. Rev. Lett. **75**,
17 (1995);
K.S. Babu and R.N. Mohapatra, Phys. Rev. Lett. **75**, 2276 (1995).
- [6] B. Brahmachari and P. Roy, Phys. Rev. **D50**, R39 (1994).
- [7] J.L. Goity and M. Sher, Phys. Lett. **B346**, 69 (1995),
D. Chang and W.-Y. Keung, Phys. Lett. **B389**, 294 (1996).
- [8] F. Zwirner, Phys. Lett. **B132**, 103 (1983).
- [9] R. Barbieri and A. Masiero, Nucl. Phys. **B267**, 679 (1986).
- [10] G. Bhattacharyya, D. Choudhury and K. Sridhar, Phys. Lett. **B355**, 193 (1995).

- [11] R. Barbieri, A. Strumia, Z. Berezhiani, Phys. Lett. **B407**, 250 (1997).
- [12] K. Choi, E.J. Chun, and K. Hwang, hep-ph/0004101; Y.Y Keum and O.C.W. Kong, hep-ph/0004110.
- [13] S.M. Barr and A. Zee, Phys. Rev. Lett. **65**, 21 (1990);
 D. Chang, W.-Y. Keung, and T.C. Yuan, Phys. Rev. **D43**, 14 (1991);
 R. G. Leigh, S. Paban and R. M. Xu, Nucl. Phys. **B352**, 45 (1991);
 C. Kao and R.-M. Xu, Phys. Lett. **B296**, 435 (1992).
- [14] D. Bowser-Chao, D. Chang and W.-Y. Keung, Phys. Rev. Lett. **79**, 1988 (1997).
- [15] D. Chang, W.-F. Chang and W.-Y. Keung, Phys. Lett. **B478** 239 (2000); hep-ph/9910465.
- [16] A. Pilaftsis, Phys. Lett. **B471**, 174 (1999).
- [17] D. Chang, W.-Y. Keung, and T.C. Yuan, Phys. Lett. **B251**, 608 (1990);
 D. Chang, W.-Y. Keung, C.S. Li and T.C. Yuan, Phys. Lett. **B241**, 589 (1990);
 J.F. Gunion and D. Wyler, Phys. Lett. **B248**, 170 (1990).
- [18] R. Arnowitt, J. L. Lopez and D. V. Nanopoulos, Phys. Rev. **D42**, 2423 (1990).
- [19] P.G. Harris et al., Phys. Rev. Lett. **82** 904 (1999).
- [20] K. Abdullah et al., Phys. Rev. Lett. **65**, 2340 (1990); E. Commins et al., Phys. Rev. **A 50**, 2960 (1994); B.E. Sauer, J. Wang and E.A. Hinds, Phys. Rev. Lett. **74**, 1554 (1995); *J. Chem. Phys* **105**, 7412 (1996).

Figure Captions

- Fig. 1
- a. (i) Rainbow-like diagram for the d quark. The generic \mathcal{R} vertex is marked by \circ and its complex conjugate by \bullet . (ii) Rainbow-like diagram for the u quark.
 - b. (i) Overlapping diagram for the d quark using λ' . (ii) Overlapping diagram for the u quark using λ' .
 - c. (i) Tent-like diagram for the d quark using λ' . (ii) Tent-like diagram for the u quark using λ' .
 - d. Barr-Zee type graph for u quark EDM

Fig. 2 A typical two-loop diagram of the Barr-Zee type. Note that there are 3 ways to insert mass.

Fig. 3 The neutron EDM D_n versus $M_{\tilde{\nu}}$ with $\sum_i \text{Im}(\lambda'_{i33} \lambda'_{i11})$ or $\sum_i \text{Im}(\lambda'_{i33} \lambda'_{i11})$ scaled to 10^{-5} .

Fig. 4 The electron EDM d_e versus $M_{\tilde{\nu}}$.